

Coupled transport of PAH and surfactants in natural aquifer material

J. Danzer¹ and P. Grathwohl¹

Applied Geology, Geological Institute, University of Tuebingen

¹ Sigwartstr. 10, D-72076 Tuebingen, Germany

Received May 1997 - Accepted October 1997

Abstract. Surfactants in aqueous solution adsorb onto mineral surfaces and form micelles above the critical micelle concentration (CMC) due to their physico-chemical properties. Hydrophobic organic compounds such as polycyclic aromatic hydrocarbons (PAHs) have a high affinity for the adsorbed surfactant layers (monomers, hemimicelles and admicelles) and to the micelles in the mobile aqueous phase. The transport of PAHs is controlled by the concentration of the surfactant and the partition coefficients, of the PAHs between water and admicelles (adsolubilization: K_{adm}) and water and micelles (solubilization: K_{mic}), respectively. These partition coefficients were measured in laboratory batch and column experiments using phenanthrene as a chemical probe for the PAHs, a non-ionic surfactant (Terrasurf G50), natural aquifer sand (River Neckar Alluvium: RNA) and its petrographic subcomponents. The sorption of the surfactant can be described by a linear isotherm for concentrations below the CMC and a sorption maximum above the CMC, which both depend on the grain size and the surfactant accessible internal surface area of the particles. K_{adm} was found to be higher than K_{mic} . Both depend on the surfactant's properties, such as alkyl chain length, polar headgroup or ethoxylation. In column experiments an increasing retardation of phenanthrene was observed up to the CMC followed by a facilitated transport at surfactant concentration several times the CMC.

1 Introduction

The transport of hydrophobic organic contaminants (HOCs) in the subsurface environment poses a serious threat to groundwater resources. Drinking water standards are very low for many HOCs, e.g. polycyclic aromatic hydrocarbons (PAHs) due to their toxic, carcinogenic and mutagenic

potential. These compounds, even at minor concentrations, impose a serious risk on groundwater quality.

The sources of HOCs in many cases are nonaqueous phase liquids (NAPL) present as pools or residual phase in the aquifer (e.g. tar-oil at former manufactured gas plant sites). Since the release of HOCs from NAPL and the desorption of HOCs from the aquifer material is limited by slow aqueous diffusion (Grathwohl and Reinhard, 1993; Pyka, 1994), existing subsurface remediation techniques, e. g. "pump and treat", require very long time periods and high operating costs.

Recently, surfactant enhanced in-situ subsurface remediation technologies, based on specific interactions between surfactants and NAPL, have been evaluated. These interactions include (i) surfactant-induced reduction of interfacial tension in order to mobilize the nonaqueous phase ("mobilization", Pennell et al., 1994), (ii) bulk extraction of nonaqueous phase liquids by ultra-low interfacial tension associated with the formation of microemulsions (Shiau et al., 1996), (iii) micellar "solubilization" to enhance desorption and transport of HOCs during soil flushing (Edwards et al., 1994, Yeom et al., 1995) and (iv) sorption of surfactants onto solids for enhancing HOC sorption and immobilization to establish in-situ treatment zones using cationic surfactants (Burris and Antworth, 1992, Wagner et al., 1994, Li and Bowman, 1997) or using surfactants below their Krafft temperature (Nayyar et al., 1994).

This study focuses on both the micellar facilitated transport and the enhanced retardation of HOC due to surfactant coated mineral surfaces. In a further study the identified processes and quantified parameters were used in a multicomponent transport model for the simulation of the coupled transport of PAH and surfactants in porous media (Finkel et al., 1997).

Correspondence to: J. Danzer

2 Background

Figure 1 summarizes the most relevant processes for the transport of HOC and surfactant in natural aquifer material. The surfactant can exist in the aqueous phase as dissolved monomers and above a surfactant specific concentration called the critical micelle concentration (CMC) as aggregated groups of molecules ("micelles"). Surfactant monomers also agglomerate at the solid/water interface and form monolayers ("hemimicelles") and bilayers ("admicelles") depending on the surfactant concentration.

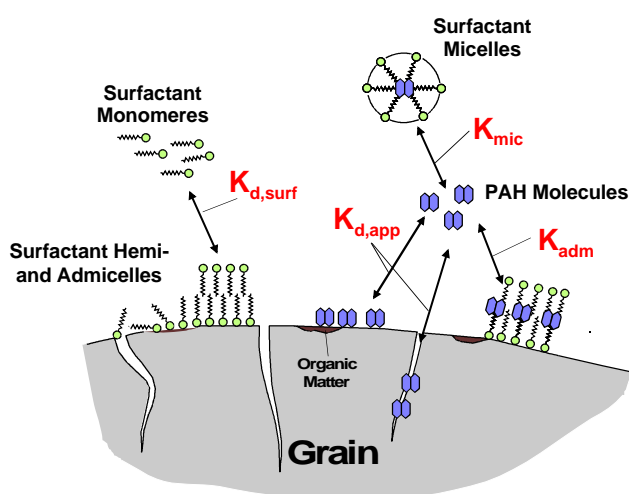


Fig. 1. Coupled transport of PAH and surfactants in natural aquifer material - conceptual model

HOCs in such a system are dissolved in the water, associated with monomers or solubilized in the micelles as well as sorbed directly onto the aquifer material and associated to admicelles. Solubilization is due to the partitioning of HOC between micelles and aqueous phase and can be quantified by a partition coefficient K_{mic} . Similarly, the partitioning of HOC between sorbed surfactants (monomers, hemimicelles and admicelles) and aqueous phase ("adsolubilization") is given by K_{adm} . The sorption of HOC to the aquifer material is mainly controlled by the organic matter content and exhibits slow kinetics due to intraparticle and intra-organic matter diffusion. Under non-equilibrium conditions it can be quantified by an apparent, time dependent distribution coefficient $K_{d,app}$. The transport velocity of HOC in the presence of surfactants relative to the groundwater velocity (conservative tracer) is referred to as retardation and is given by a dimensionless retardation factor R_d . It can be expressed as the ratio of the total mass of HOC in the porous medium to the mass in the mobile phase (Eq. 1):

$$R_d = 1 + \frac{r_b}{n} \cdot \frac{K_{d,app} + K_{adm} \cdot q}{1 + K_{mic} \cdot C_{mic}} \quad (1)$$

Besides the properties of the porous medium (bulk density r_b and effective porosity n) the retardation of the HOC depends on the partition coefficients $K_{d,app}$, K_{adm} and K_{mic} as well as on the behavior of the surfactant described by the adsorbed surfactant concentration q and the concentration of the micelles C_{mic} . Micelles are not present at surfactant concentrations below the CMC and the retardation increases with increasing sorbed surfactant concentration q . Above the CMC a maximum adsorbed surfactant concentration q_{max} is reached, micelles are formed, and the retardation decreases with increasing micelle concentration.

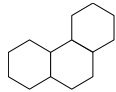
3 Materials and Methods

Adsorption isotherms were measured in batch systems for different aquifer materials under equilibrium conditions. CaCl_2 was added to a final concentration of 0.01 M to provide an equal ionic strength in all batch systems. Surfactant breakthrough curves were obtained by column experiments under non-equilibrium conditions using a fraction collector. Since surfactant concentrations were well above background concentration of dissolved organic carbon, all surfactant concentrations were measured as total organic carbon (TOC) in the aqueous phase using a TOC-analyzer (highTOC, elemental, Germany).

Partitioning of phenanthrene between adsorbed surfactant and aqueous phase (adsolubilization) was measured in batch systems under equilibrium conditions using HPLC-fluorescence detection of phenanthrene. The coupled transport of phenanthrene and surfactant was examined in breakthrough experiments using an on-line fluorescence detection (Fig. 2). Since the fluorescence of phenanthrene was not influenced by quenching effects in the presence of surfactant, the detected signal was not corrected. In the experimental setup only stainless steel and glass components came in contact with the phenanthrene and a constant flow and temperature could be maintained. Fluorescein was used as a conservative tracer to obtain hydrodynamic parameters such as effective pore volumes and dispersion coefficients for each column experiment. The properties of the used columns are given in the respective figure captions.

Tables 1 and 2 show physico-chemical properties of phenanthrene (used as a chemical probe for the PAH) and the nonionic surfactant Terrasurf G50 (ethoxylated fatty alcohol). Table 3 shows the properties of the natural aquifer material River Neckar Alluvium (RNA) and its petrographic subcomponents which were obtained by visual separation of RNA. Different grain size fractions were obtained by sieving.

Table 1. Physico-chemical properties of phenanthrene

Compound (Formula)	Structure	Molecular Weight [g/mol]	Vapor Pressure [torr] (20°C)	Water Solubility [mg/L] (25°C)		log K_{ow} [-]	
Phenanthrene (C ₁₄ H ₁₀)		178	$6.80 \cdot 10^{-4}$	1.29 ^a	1.18 ^b	4.63 ^b	4.57 ^c 4.46 ^d

^a Mackay and Shiu, (1977), ^b Yalkowsky and Valvani, (1979), ^c Miller and Wasik, (1985), ^d Sims and Overcash, (1983)

Table 2. Characteristics of the surfactant used in this study

Surfactant	Type	Formula ^c	Molecular Weight ^c [g/mol]	CMC ^d [mg/L]	HLB ^e [-]
Terrasurf G50 (Dow Chemicals)	ethoxylated fatty alcohol (nonionic)	I ^a -EO ^b 8	570	500	12.9

^a initial fatty alcohol, ^b grade of ethoxylation, ^c average value, ^d critical micelle concentration in pure water determined by a surface tension method, ^e hydrophilic lipophilic balance

Table 3. Characteristics of River Neckar Alluvium (RNA)

Aquifer Material	Subcomponent	Grain Size [mm]	f _{oc} ^a [%]	CaCO ₃ ^b [%]	BET Surface Area ^c [m ² /g]	Pore- \bar{r} ^d [nm]
RNA	bulk sample	0.25 - 1.0	0.0525 ± 0.0048	24.97	8.68	n. d.
RNA	bulk sample	2.0 - 4.0	0.0725 ± 0.0017	84.02	n. d. ^e	n. d.
RNA - JK	Jurassic limestones	2.0 - 4.0	0.0747 ± 0.0023	88.85	3.51	49
RNA - MSK	Triassic limestones	2.0 - 4.0	0.1274 ± 0.0047	87.73	1.32	54
RNA - SS	sandstones	2.0 - 4.0	0.0721 ± 0.0017	0.50	4.21	107
RNA - Qz	quartz	2.0 - 4.0	0.0058 ± 0.0013	< 0.2	0.15	n. d.

^a organic carbon content (determined by combustion and infrared detection of CO₂), ^b calcium carbonate content, ^c determined by N₂ adsorption/desorption isotherms, ^d pore diameter determined by comparison of surfactant adsorption and Hg porosimetry data, ^e not determined

4 Results

4.1 Surfactant transport

A typical surfactant isotherm of Terrasurf G50 onto RNA is shown in Fig. 3. Although in the literature mostly a Langmuir type adsorption model is used to describe surfactant adsorption, a much better fit is obtained by a linear isotherm below the CMC followed by a maximum sorption q_{max} . In that case following relationship between q_{max} , $K_{d, surf}$ and CMC exists: $q_{max} = K_{d, surf} CMC$. It should be noted that the CMC obtained from the adsorption isotherm ($CMC = q_{max} K_{d, surf}^{-1}$) is decreased due to the presence of electrolyte (0.01 M CaCl₂) compared to the

CMC determined by the change of surface tension in pure water.

RNA is a heterogeneous aquifer material with low organic carbon content. It consists of Triassic limestones, Jurassic limestones, different sandstones and quartz in different mass percentages depending on the grain size. The grain size fraction 2 mm - 4 mm was separated into its lithological subcomponents to identify their influence on surfactant sorption. The isotherms of the subcomponents (Fig. 4) also show a non-linear shape with highest $K_{d, surf}$ and q_{max} values for the sandstones followed by Jurassic and Triassic limestones and the lowest values for quartz.

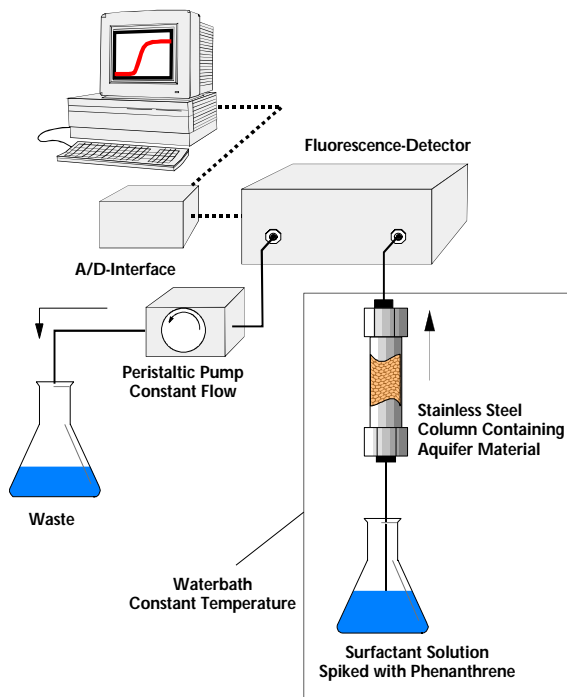


Fig. 2. Experimental setup for the on-line detection of phenanthrene breakthrough curves in the presence of surfactant

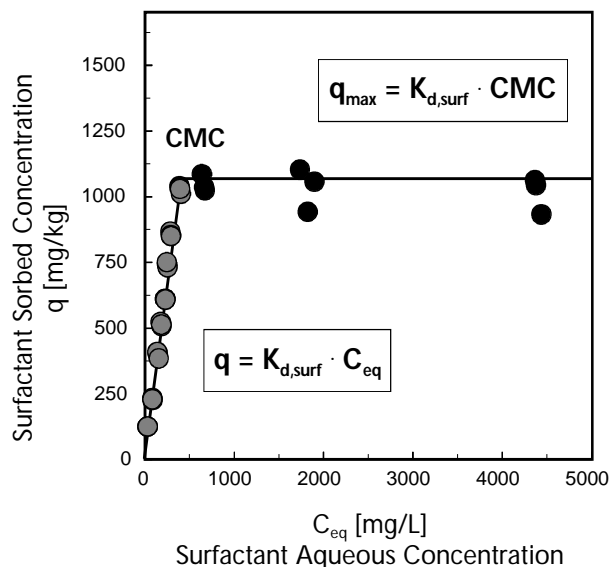


Fig. 3. Adsorption isotherm of nonionic surfactant Terrasurf G50 onto River Neckar Alluvium (grain size 0.25 mm - 1.0 mm)

This can be explained by the internal surface of the particles, which is accessible to surfactant molecules in addition to the exterior surface.

The accessibility of the internal surface depends on the intraparticle pore size distribution. Sandstones mainly have macropores, the Jurassic limestones have some mesopores, the Triassic limestones have also micropores < 2 nm and Quartz has almost no intraparticle porosity. The surface area was calculated from the surfactant adsorption assuming a complete surfactant bilayer coverage at q_{max} and using the

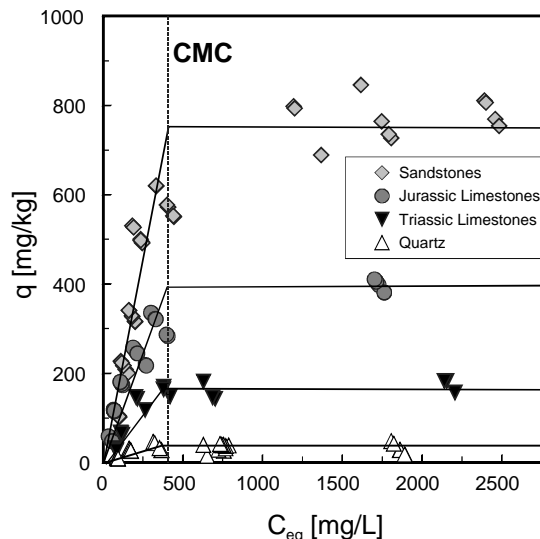


Fig. 4. Adsorption isotherms of Terrasurf G50 onto petrographic sub-components of RNA (grain size 2 mm - 4 mm)

measured surface area which is covered by one surfactant molecule (44 \AA^2). The area determined was compared with the specific surface area using nitrogen and mercury adsorption and desorption (Tab. 3). It indicates that Terrasurf G50 reaches surfaces in macropores between 50 nm and 100 nm.

Since adsorption sites at the external surface seem to be easily accessible by the surfactant, the grain size of the aquifer material is an important parameter beside the lithological composition. Figure 5 shows this for Quartz and Triassic limestones. This does not apply for the macroporous sandstone fragments. If the maximum surfactant adsorption onto the aquifer material is known, the surfactant loss occurring in a surfactant enhanced subsurface remediation can be calculated.

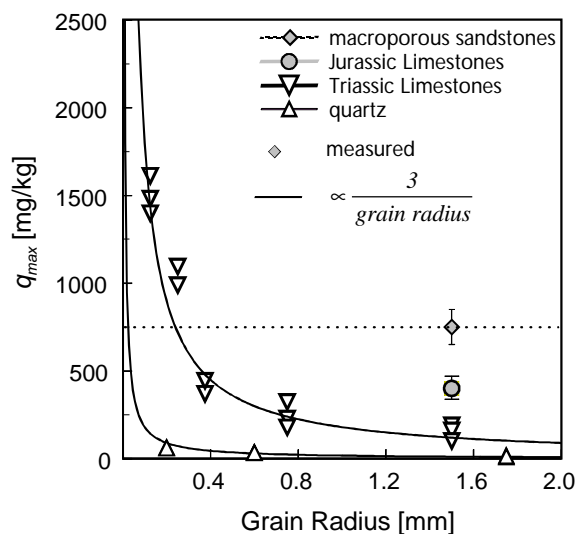


Fig. 5. Maximum adsorption q_{max} of Terrasurf G50 depending on the grain size of different petrographic sub-components of RNA. Lines calculated according to the decreasing surface/volume ratio of spheres versus grain radius

Figure 6 shows a typical breakthrough curve of the surfactant transport in a saturated column experiment. The breakthrough of the surfactant can be described reasonably well by an analytical solution of the advection dispersion equation based on a local equilibrium assumption (Ogata and Banks, 1961). A small tailing, due to slow diffusion into intragranular pores and reorientation of the surfactant bilayer, could be observed.

A further stepwise increase of the surfactant concentration above CMC (q_{max} established) is not retarded in the column as expected from the shape of the sorption isotherm. After equilibration with the higher inflow concentration the column was flushed with pure water and the surfactant was completely desorbed, indicating that the surfactant adsorption is reversible.

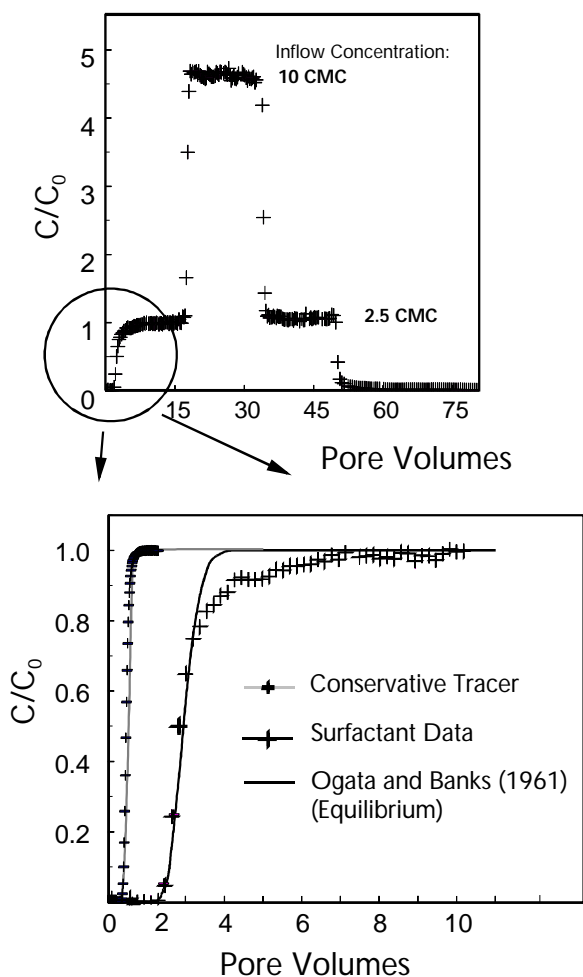


Fig. 6. Surfactant breakthrough curves of Terrasurf G50 through RNA (0.25 mm - 1.0 mm), "two step" - adsorption and desorption. It should be noted that for concentrations above the CMC no further retardation occurs. Column length 9 cm, column diameter 1 cm, flow velocity ≈ 8 m/day, bulk density $\rho_b = 1.8$ g/cm³, effective porosity $n = 0.34$, surfactant inflow concentration $C_0 = 2.5$ CMC (first step) and $C_0 = 10$ CMC (second step), conservative tracer: Fluorescein

4.2 Coupled transport of PAH and surfactant

The partitioning of phenanthrene between admicelles and the aqueous phase was measured under equilibrium conditions in batch systems containing aquifer material and surfactant. The surfactant concentration was close to the CMC at which all adsorbed surfactant molecules are assumed to form admicelles. Figure 7 shows isotherms of phenanthrene onto RNA without surfactant and in the presence of surfactant. The slope of the linear isotherm in the absence of surfactant gives the apparent distribution coefficient $K_{d, app}$ since sorption onto RNA did not reach equilibrium due to the intraparticle diffusion limitations. The slope of the isotherm for the aquifer material coated with surfactant is about five times steeper, resulting in a higher distribution coefficient. The partition coefficient of phenanthrene between admicelles and water (K_{adm}) was found to be about 18300 L/kg for Terrasurf G50, which is about 35 % of the octanol/water partition coefficient K_{ow} . These results are in good agreement with data reported by Sun and Jaffé (1996), who examined phenanthrene adsorption onto aluminum oxide coated with di-anionic surfactants (DOWFAX). They found values of K_{adm} between 16600 L/kg and 32100 L/kg and values of K_{mic} between 4000 L/kg and 11000 L/kg depending of the alkyl chain length of the used surfactant.

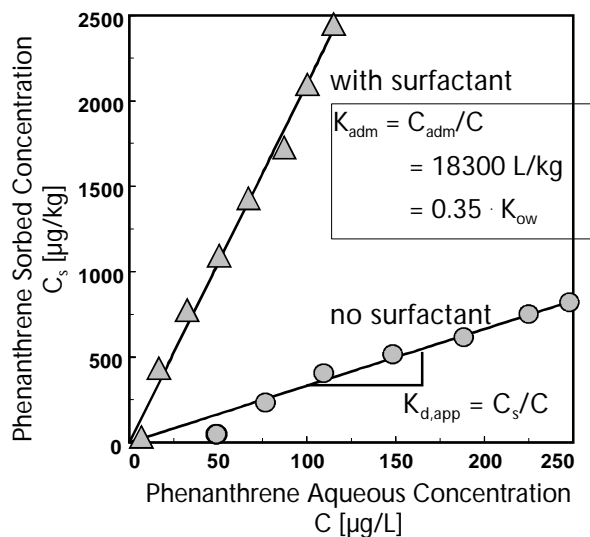


Fig. 7. Adsorption isotherms of phenanthrene with and without surfactant. $K_{d, app}$: apparent distribution coefficient (non-equilibrium due to the diffusion limited intraparticle pore diffusion); K_{adm} : phenanthrene partition coefficient between admicelles and aqueous phase

The on-line measured breakthrough curves of phenanthrene are shown in Fig. 8. The retardation of phenanthrene increases with increasing surfactant concentration up to the CMC. Above the CMC the retardation decreases with

increasing surfactant concentration. The same retardation compared to the system without surfactant is reached at concentrations about 10 times the CMC.

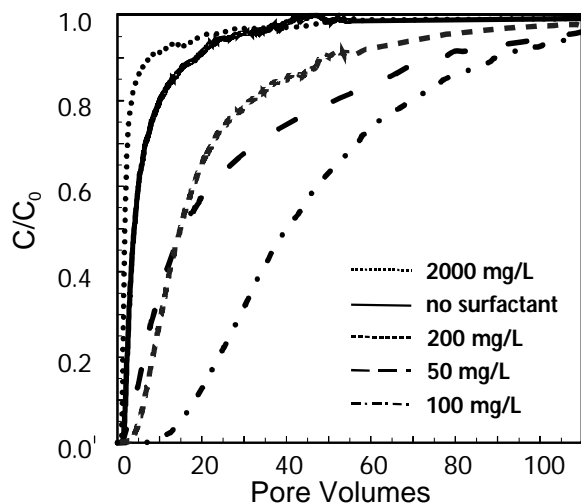


Fig. 8. Breakthrough curves of phenanthrene through RNA packed columns at different surfactant concentrations of Terrasurf G50. The transport of phenanthrene without surfactant is given by the solid line. Column length 12 cm, column diameter 2.5 cm, RNA grain size 1.0 mm - 2.0 mm, $\rho_b = 1.8 \text{ g/cm}^3$, effective porosity $n \approx 0.34$, flow velocity $\approx 8 \text{ m/day}$, phenanthrene inflow concentration $C_0 = 100 \text{ }\mu\text{g/L}$, Fluorescence on-line detection, CMC $\approx 100 \text{ mg/L}$

The retardation factors were determined by the ratio of the areas above the breakthrough curves of phenanthrene and the conservative tracer. It may be noted that the CMC in these experiments is less than reported in Table 2, which is believed to be due to small amounts of methanol in which phenanthrene was spiked to the water. The partition coefficient of phenanthrene between micelles and the aqueous phase K_{mic} was determined by fitting this parameter in the mass balance model according to Eq. 1 to measured retardation factors (Fig. 9). K_{mic} was found to be about half the value of K_{adm} , which may be due to following reason: The micelles have a larger hydration layer which is mainly around the hydrophilic exterior of the micelle. The thickness of this hydration layer may be decreased if temporary charges of the hydrophilic headgroups are neutralized when the surfactant is sorbed to the solid. This would result in an increase in the hydrophobic interactions of surfactant bilayers with phenanthrene molecules (Sun and Jaffé, 1996).

As shown in Fig. 10, retardation factors can be predicted reasonably well, if K_{adm} , K_{mic} , $K_{d, app}$, q and C_{mic} are known from independent measurements. The maximum retardation factor achieved is about 35. An enhanced retardation can be observed up to concentrations 10 times the CMC and a facilitated transport of phenanthrene takes place above that concentration.

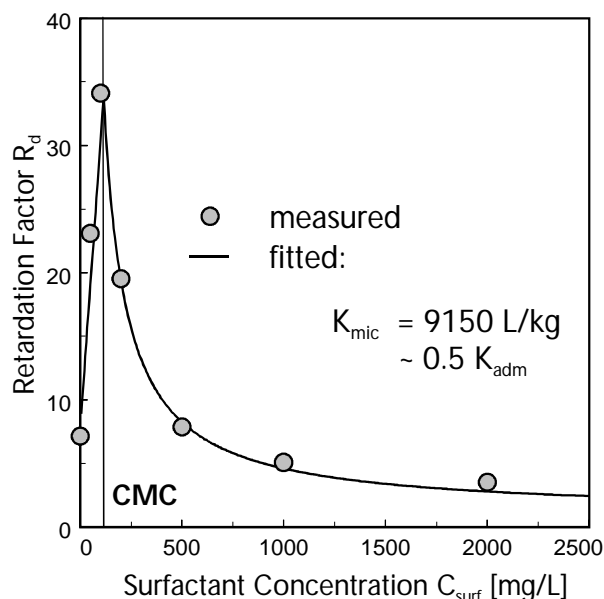


Fig. 9. Retardation factors of phenanthrene determined from breakthrough curves (Fig. 8) at different surfactant concentrations (Terrasurf G50). The solid line was calculated according to Eq. 1 using $K_{d, app} = 1.2 \text{ L/kg}$, $K_{adm} = 18300 \text{ L/kg}$, $K_{d, surf} = 2.34 \text{ L/kg}$, $q = K_{d, surf} C_{surf}$ and K_{mic} as fitting parameter

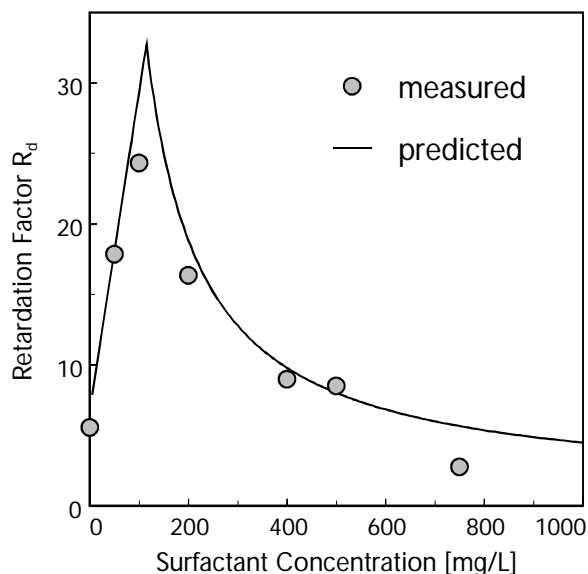


Fig. 10. Prediction of retardation factors of phenanthrene at different surfactant concentrations using data shown in Fig. 9. Terrasurf G50, 0.25 mm - 1.0 mm RNA, column length 9 cm, column diameter 1 cm, flow velocity $\approx 25 \text{ m/day}$, bulk density $\rho_b = 1.8 \text{ g/cm}^3$, effective porosity $n \approx 0.35$, phenanthrene inflow concentration $C_0 = 50 \text{ }\mu\text{g/L}$, CMC $\approx 100 \text{ mg/L}$, $K_{d, app} = 1.087 \text{ L/kg}$, $K_{adm} = 18300 \text{ L/kg}$, $K_{mic} = 9150 \text{ L/kg}$, $K_{d, surf} = 2.34 \text{ L/kg}$, $q = K_{d, surf} C_{surf}$

5 Summary

Batch and column experiments were conducted in the laboratory to examine the transport of surfactants and the coupled transport of PAH and surfactants in natural aquifer material. It was found that the surfactant isotherm can be described by two linear parts: a linear isotherm below the CMC and a sorption maximum above the CMC. The adsorption of the surfactant depends on the grain size and the petrographic properties (e.g. macropore and mesopore distribution, internal accessible surface area) of the aquifer material.

The coupled transport of PAH and surfactants can be described by a retardation factor which depends on the surfactant concentration and adsorption and the partitioning of phenanthrene between the immobile surfactant phase, the mobile micelles and the aqueous phase. Enhanced retardation was observed for concentrations up to about 10 times the CMC and a facilitated transport above that concentration.

Acknowledgements. This study was funded by the State of Baden-Württemberg (PWAB PD-94 160).

References

- Burris, D. R., Antworth, C. P. (1992), In situ modification of an aquifer material by a cationic surfactant to enhance retardation of organic contaminants, *J. Contam. Hydrol.* 10, 325-337.
- Edwards, D.A., Liu, Z. and Luthy, R.G. (1994), Experimental data and modeling for surfactant micelles, HOCs, and Soil, *J. Environ. Eng.* 120, 23-41.
- Finkel, M., Liedl, R., Teutsch, G. (1997), Modeling surfactant influenced PAH migration, *Physics and Chemistry of the Earth, this issue.*
- Grathwohl, P., Reinhard, M. (1993), Desorption of trichlorethylene in aquifer material. Rate limitations at the grain scale, *Environ. Sci. Technol.* 27 (12) 2360-2366.
- Li, Z.H., Bowman, R. S (1997), Counterion effects on the sorption of cationic surfactant and chromate on natural clinoptilolite. *Environ.Sci.Technol.* 31(8), 2407-2412.
- Mackay, D. Shiu, W.J. (1977), Aqueous solubility of polynuclear hydrocarbons, *J. Chem. Eng. Data*, 22 (4), 399-402.
- Miller, M.M., Wasik, S. P. (1985), Relationship between octanol-water partition coefficient and aqueous solubility, *Environ. Sci. Technol.* 19 (6), 522-529.
- Nayyar, S. P., Sabatini, D. A., Harwell, J. H. (1994), Surfactant adsolubilization and modified sorption of nonpolar, polar and ionizable organic contaminants, *Environ. Sci. Technol.* 28, 1874 - 1881.
- Ogata, A., Banks, R.G. (1961), A solution of the differential equation of longitudinal dispersion in porous media, *U.S. Geological Survey Professional Paper* 411-A, Washington D.C.
- Pennell, K.D., Jin, M., Abriola, L.M. and Pope, G.A. (1994), Surfactants enhanced remediation of soil columns contaminated by residual tetrachloroethylene, *J. Contam. Hydrol.* 16, 35-53.
- Pyka, W. (1994), Freisetzung von Teer Inhaltsstoffen aus residualer Teerphase in das Grundwasser, Laboruntersuchungen zur Lösungsrate und Lösungsvermittlung, *Tübinger Geowissenschaftliche Arbeiten, Reihe C*, Nr. 21, 76 S., Tübingen.
- Shiau, B.-J., Sabatini, D. A., Harwell, J. H., Vu. D. Q. (1996), Microemulsion of mixed chlorinated solvents using food grade (edible) surfactants, *Environ. Sci. Technol.* 30 (1), 97-103.
- Sims, R.C., Overcash, M.R. (1983), Fate of polynuclear aromatic compounds (PNA) in soil-plant systems, *Residue Reviews*, Vol. 88, Springer Verlag N.Y. Inc., 1-68.
- Sun, S., Jaffé, P. R. (1996), Sorption of phenanthrene from water onto alumina coated with dianionic surfactants, *Environ. Sci. Technol.* 30, 2906-2913.
- Wagner, J., Chen, H., Brownawell, B.J., and Westall, J.C. (1994), Use of cationic surfactants to modify soil surfaces to promote sorption and retard migration of hydrophobic organic compounds. *Environ. Sci. Technol.* 28, 231-237.
- Yalkowsky, S.H., Valvani, S.C. (1979), Solubilities and partitioning - 2. Relationships between aqueous solubilities, partition coefficients and molecular surface areas of rigid aromatic hydrocarbons, *J. Chem. Eng. Data* 24 (2), 127-129.
- Yeom, I.T., Ghosh, M.M., Cox, C.D., Robinson, K.G. (1995), Micellar solubilization of polynuclear aromatic hydrocarbons in coal tar-contaminated soils, *Environ. Sci. Technol.* 29, 3015-3021.